Specification of a Two-Dimensional Test Case

(IEA)

Nielsen, Peter Vilhelm

Publication date:
1990

Document Version
Publisher's PDF, also known as Version of record

INSTITUTTET FOR BYGNINGSTEKNIK
DEPT. OF BUILDING TECHNOLOGY AND STRUCTURAL ENGINEERING
AALBORG UNIVERSITETSCENTER • AUC • AALBORG • DANMARK

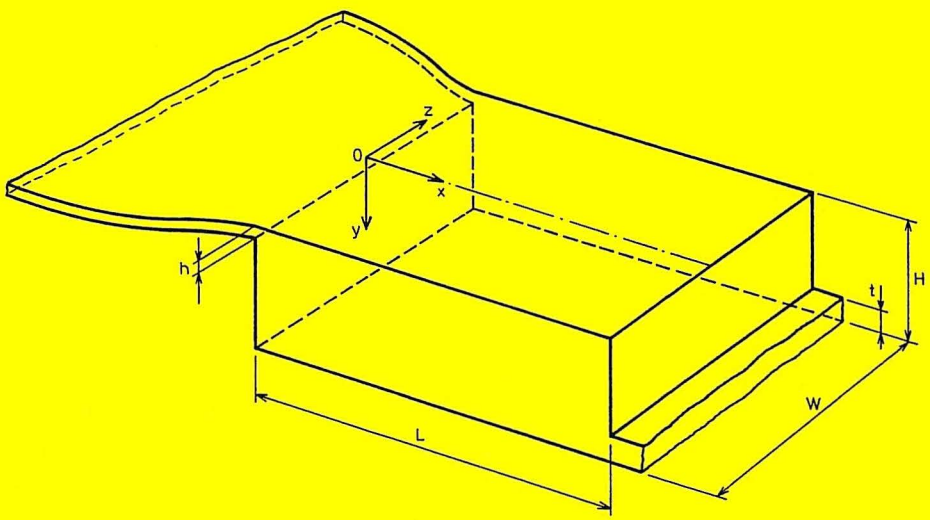

International Energy Agency, Energy Conservation in Buildings and Community Systems, Annex 20: Air Flow Pattern Within Buildings

PETER V. NIELSEN
SPECIFICATION OF A TWO-DIMENSIONAL TEST CASE
NOVEMBER 1990 ISSN 0902-7513 R9040

Printed at Aalborg University

INSTITUTTET FOR BYGNINGSTEKNIK
DEPT. OF BUILDING TECHNOLOGY AND STRUCTURAL ENGINEERING
AALBORG UNIVERSITETSCENTER • AUC • AALBORG • DANMARK

International Energy Agency, Energy Conservation in Buildings and Community Systems, Annex 20: Air Flow Pattern Within Buildings

PETER V. NIELSEN
SPECIFICATION OF A TWO-DIMENSIONAL TEST CASE
NOVEMBER 1990 ISSN 0902-7513 R9040

RESEARCH ITEM NO. 1.45
SPECIFICATION OF A TWO-DIMENSIONAL TEST CASE

Peter V. Nielsen, The University of Aalborg, Denmark

INTRODUCTION

This paper describes the geometry and other boundary conditions for a test case which can be used to test different two-dimensional CFD codes in the IEA Annex 20 work.

The given supply opening is large compared with practical openings. Therefore, this geometry will reduce the need for a high number of grid points in the wall jet region.

The geometry is suitable for test of different CFD codes because there exist a number of measurements of the flow. The geometry has also been used ealier for test of computer codes and could therefore be standardized as a benchmark test for room air distribution models.

SPECIFICATION OF ISOTHERMAL TEST CASE (case 2D1)

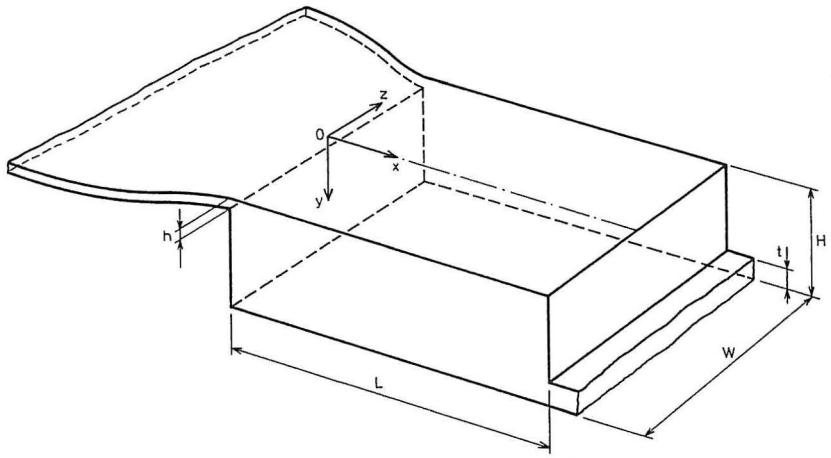

Figure 1. Model for test case and experiments. System of co-ordinates.

The geometry of the test case has the following specification, see figure 1.

$$L/H = 3.0\ ,\ h/H = 0.056\ and\ t/H = 0.16 \tag{1}$$

or

$$H = 3.0\ m\ ,\ L = 9.0\ m\ ,\ h = 0.168\ m\ and\ t = 0.48\ m \tag{2}$$

Obviously the height of the supply opening is rather large compared with practical diffusers. This geometry will reduce the need for a high number of grid points and it is possible to make an inlet specification direct at the opening instead of using the box method or the prescribed velocity method. A large opening will also ensure that the main part of the inlet flow passes outside the boundary region of the ceiling where different boundary conditions are used in CFD codes.

The inlet conditions for the velocity are given by

$$Re = \frac{h \cdot u_o}{\nu} = 5000 \tag{3}$$

or

$$u_o = 0,455\ m/s \tag{4}$$

for a kinematic viscosity of $\nu = 15{,}3 \cdot 10^{-6}$ m^2/s at an inlet temperature of 20°C. The Reynolds number is based on the slot height because the flow in the ceiling region and in the rest of the room is strongly influenced by the inlet conditions.

Inlet conditions for the turbulent kinetic energy k and dissipation ϵ are given by

$$k_o = 1.5\ (0.04 \cdot u_o)^{\ 2} \tag{5}$$

$$\epsilon_o = k_o^{1.5}/\ell_o \tag{6}$$

where

$$\ell_o = h/10 \tag{7}$$

The inlet conditions correspond to a turbulence intensity of 4%. It is difficult to stipulate ϵ_o but variation of the length scale ℓ_o within a reasonable level shows only a very small influence on the flow in the room. The production and dissipation of turbulence in the shear layer in the downstream flow will dominate the possible effect of different inlet values, see [1].

Prediction of the flow should be given at the two vertical lines

$$x = H \ , \ x = 2H \tag{8}$$

and at the two horizontal lines

$$y = h/2 \ , \ y = H - h/2 \tag{9}$$

Figures 5, 6, 7, 8 and 10 show measurements at those locations which can be used for comparison.

The isothermal test case (2D1) can be extended by a mass transport equation and constant mass flux along the floor. (This situation may be simulated by an energy equation and constant heat flux along the floor for the Archimedes number $Ar \rightarrow 0$. The buoyancy term in the Navier-Stokes equation had to be ignored). Prediction of the concentration profile should be given at the horizontal level

$$y = 0.75H \tag{10}$$

Figure 11 shows measurements at this location which can be used for comparison. The measurements were made at a Reynolds number of 7100.

The literature shows two dimensional predictions in the selected geometry. Predictions in reference [2] are based on the numerical solution of the vorticity and stream function equations and predictions in references [1], [3] and [4] are based on numerical solution of the continuity and momentum equations.

SPECIFICATION OF NON-ISOTHERMAL TEST CASE (case 2D2)

The aim of this test case is to predict flow with a strong buoyant effect. A constant heat flux is added along the floor and the Archimedes number is raised until the CFD code predicts a flow with a reduced penetration depth x_{re}.

The Archimedes number Ar is defined as

$$Ar = \frac{\beta \cdot g \cdot h \cdot \Delta T_o}{u_o^2} \tag{11}$$

where β, g and ΔT_o are volume expansion coefficient, gravitational acceleration and temperature difference between return and supply, respectively.

The prediction will be made in the same geometry and at the same velocity level as used in the isothermal case (1), (2), (3) and (4).

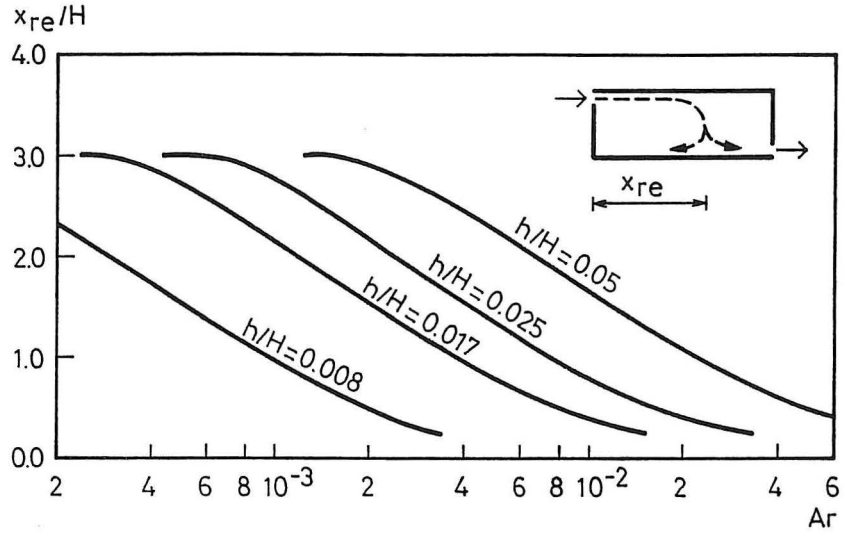

Figure 2. Penetration depths x_{re} in models with different inlet geometry.

Figure 2 shows the results of a number of model experiments made by Schwenke [5]. It is indicated that a cold supply jet will deflect from the ceiling before it reaches the end wall for a Archimedes number Ar equal to or larger than 0.02.

It should be stressed that experiments for $h/H = 0.056$ and $Re = 5000$ are missing.

A selection of $Ar = 0.02$ corresponds to a temperature difference between return and supply of

$$\Delta T_o = 0.74°C \tag{12}$$

in the geometry with room height of 3 m and a supply velocity of 0.455 m/s. The low velocity in the room ensures a buoyant flow at the given level of temperature differences.

The heat flux is calculated from $\Delta T_o, u_o$ and h.

The predictions are repeated for increasing Archimedes' number until a reduced penetration depth x_{re} takes place

$$Ar = 0.02....0.04....0.08....0.12.... \tag{13}$$

The length of the penetration depth x_{re} is in some cases dependent on the initial conditions. This is shown in reference [5] where two different x_{re} are obtained when the same measuring conditions are reached through increasing Archimedes' number and decreasing Archimedes' number. This effect can be predicted with a CFD code as shown in reference [6].

The flow field should be given in the same way as in the isothermal case, see (8) and (9).

Furthermore, a horizontal section showing the part of the jet should be given for the Archimedes number where reduced penetration takes place. A depiction of the maximum velocity u_{rm} in the occupied zone, as a function of the different Archimedes' number, will also be relevant, see figure 3 in reference [6].

LASER-DOPPLER MEASUREMENTS

The measurements described in this chapter are made by laser-doppler anemometry in a model with the geometrical specification of (1) and with $W/H = 1.0$ where W is the width of the model. The model has a real size of $H = 89{,}3$ mm. The work is a part of A. Restivo's Ph.D. thesis [1]. Laser-doppler anemometry is suitable for measuring the velocity in recirculating flow compared with hot-wire and hot sphere equipment.

Figure 3 shows the u-velocity and the intensity $\sqrt{\overline{u'^2}}$ in four different points as a function of the Reynolds number. The flow seems to be fully turbulent for a Reynolds number of 5000.

Figure 4 shows the inlet profiles. The profiles are unfortunately slightly influenced by the inlet geometry which has a contraction in the z-direction and constant height. Measurements of the rms velocity justified the value of 4% in the predictions, see (5).

Figures 5 and 6 show the mean and rms velocity at the two vertical positions $x/H = 1.0$ and 2.0. The upper part of the flow is typical for a wall jet. The figures show that the main part of the flow has a high turbulent level compared with the mean velocity which means that measurements with hot-wire anemometry would be very difficult.

The turbulent intensity $\sqrt{\overline{u'^2}}$ is the upper and lower part of the model at $x/H = 2.0$ is typical of a wall jet. The intensities in the two other directions in a two-dimensional wall jet may be given as $\overline{v'^2} \sim 0.6\ \overline{u'^2}$ and $\overline{w'^2} \sim 0.8\ \overline{u'^2}$. This means that the turbulent kinetic energy has a level rather close to the intensity $\sqrt{\overline{u'^2}}$

$$\sqrt{k} \sim 1.1\sqrt{\overline{u'^2}} \tag{14}$$

Equation (14) may be used for a rough validation of the predicted turbulent kinetic energy.

The turbulence intensity $\sqrt{\overline{u'^2}}$ in the lower part of the model at $x/H = 1.0$ is rather close to the mean velocity u which means that the turbulence is transported to this area.

Comparisons between mean velocity in figures 5 and 6 show that the flow is slightly three-dimensional. This is also recorded with hot-wire measurements given in figure 10 for $W/H = 0.5$ and 1.0.

Figures 7 and 8 show u and $\sqrt{\overline{u'^2}}$ close to the top and bottom wall. It should especially be observed that recirculating flow takes place in the corner at the wall opposite the inlet as well as in the corner below the inlet.

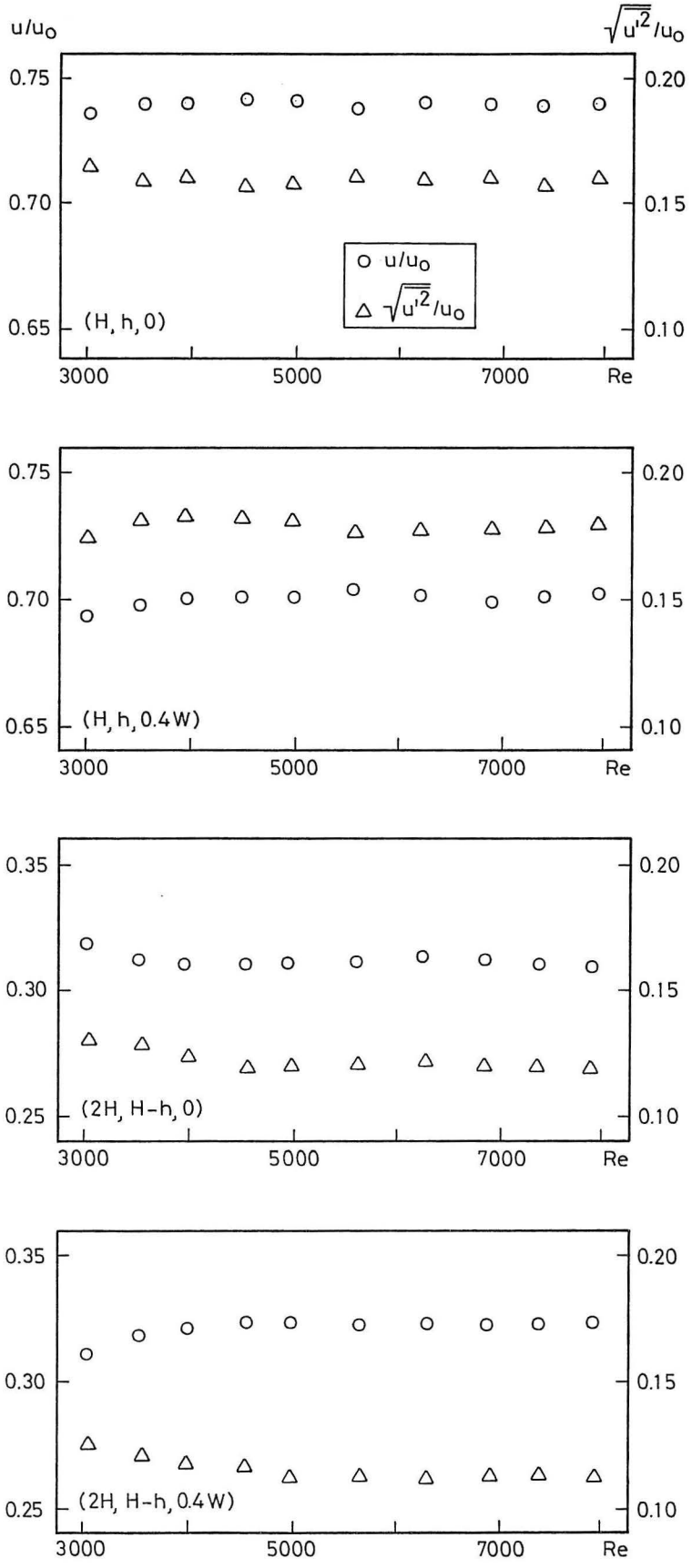

Figure 3. Dependence on mean and rms velocity on Reynolds' number, see [1].

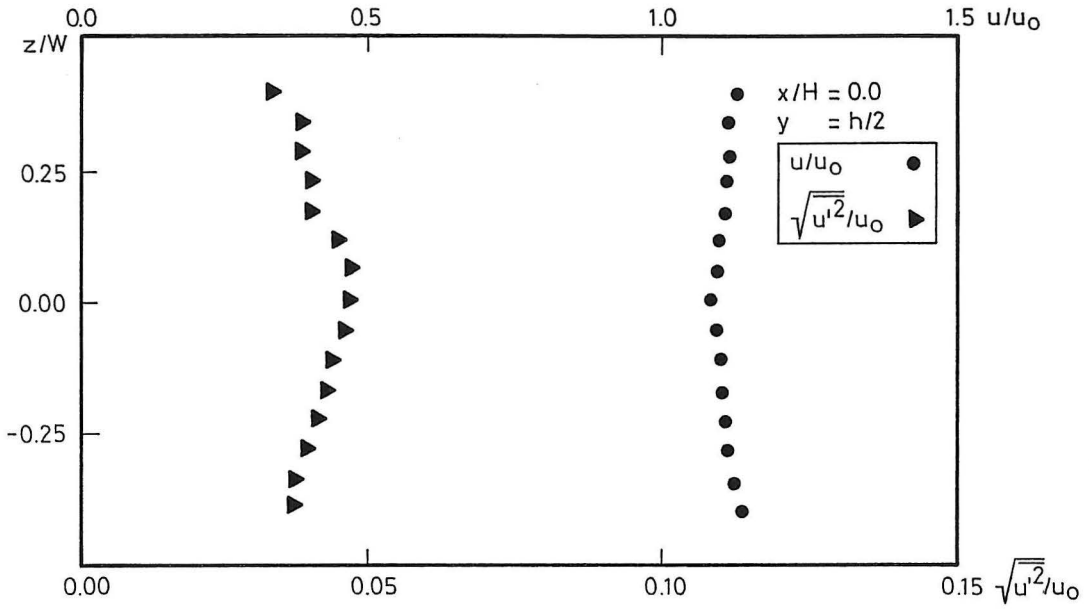

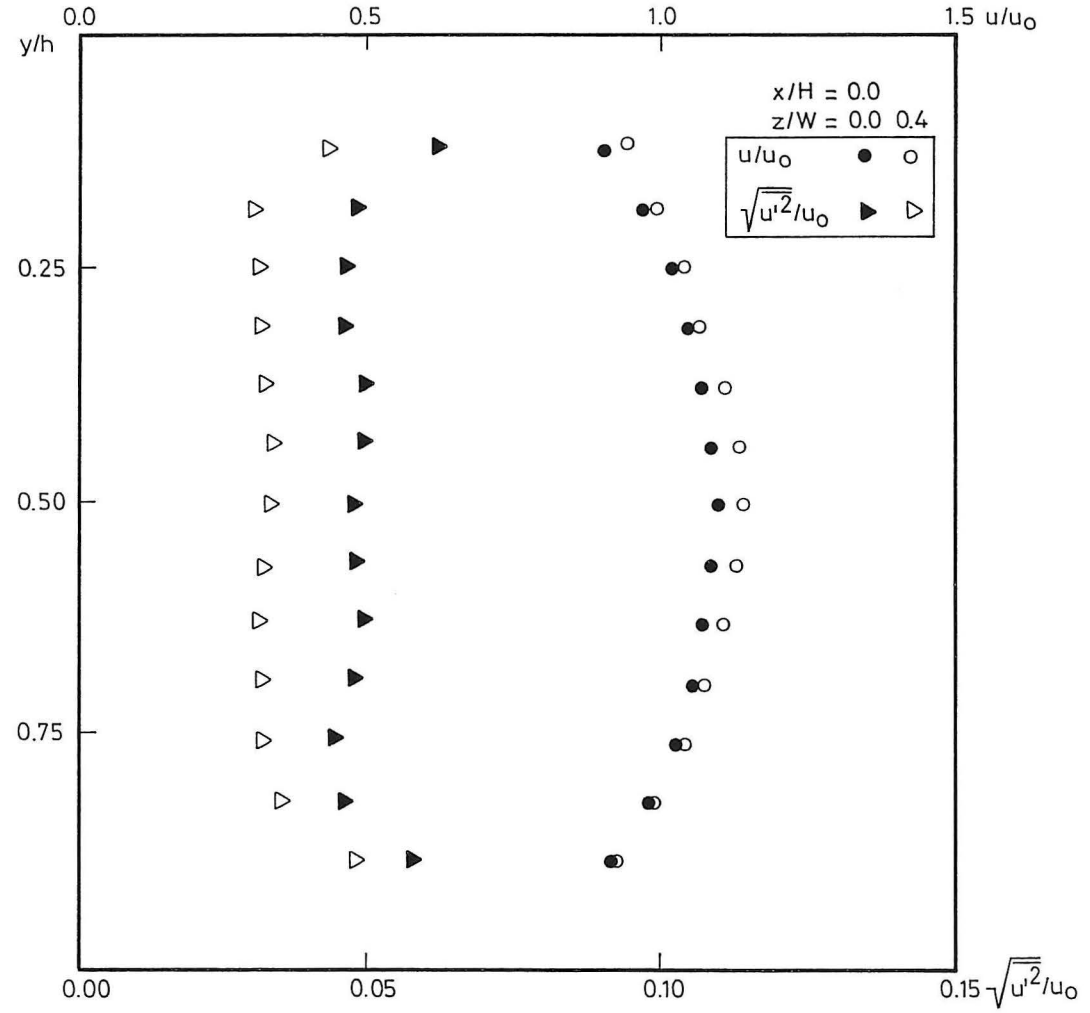

Figure 4. Inlet profiles, $Re = 5000$, see [1].

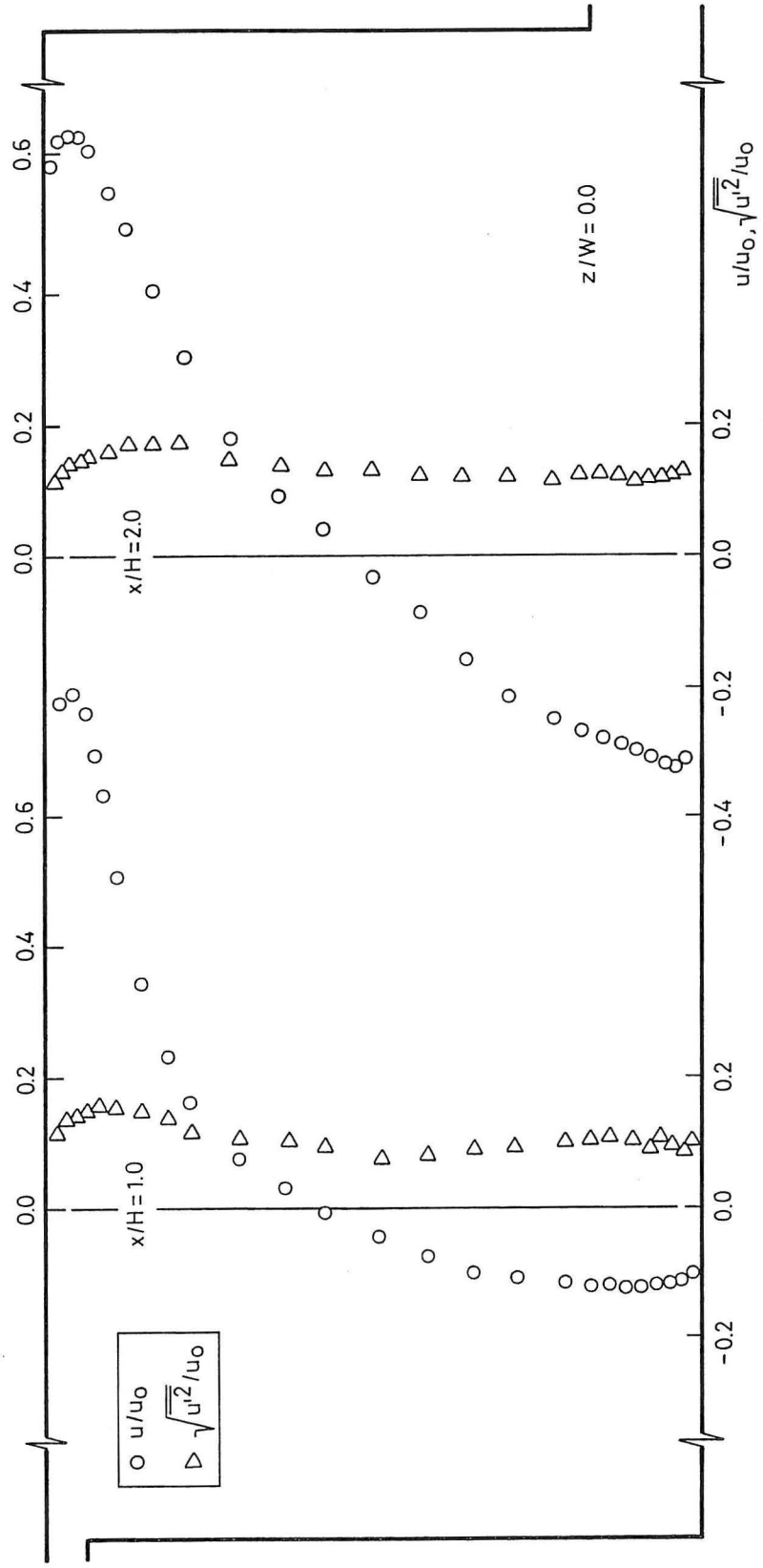

Figure 5. Measured mean and rms velocity in the symmetry plane, $Re = 5000$, see [1].

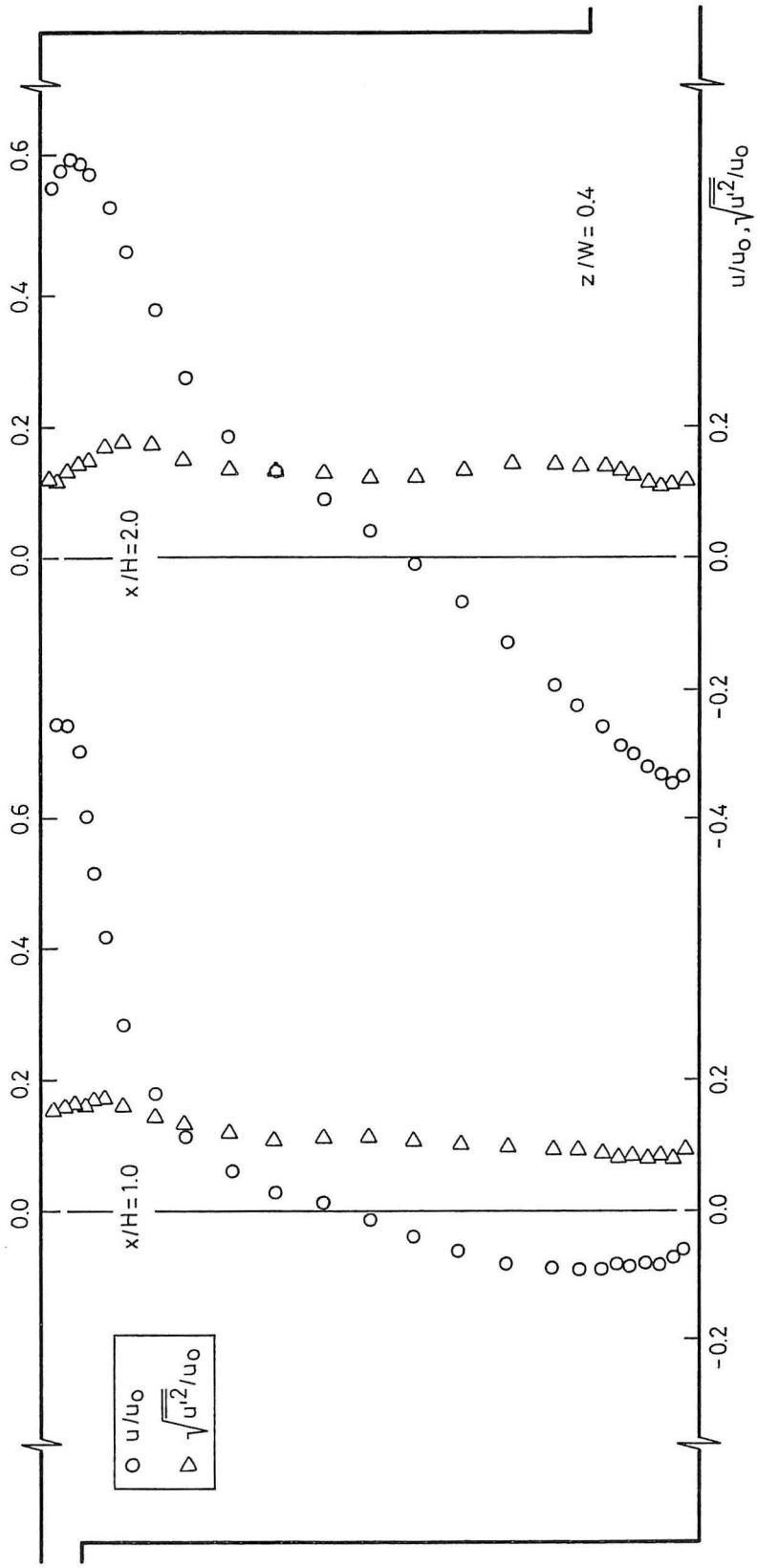

Figure 6. Measured mean and rms velocity in the plane $z/W = 0.4$, $Re = 5000$, see [1].

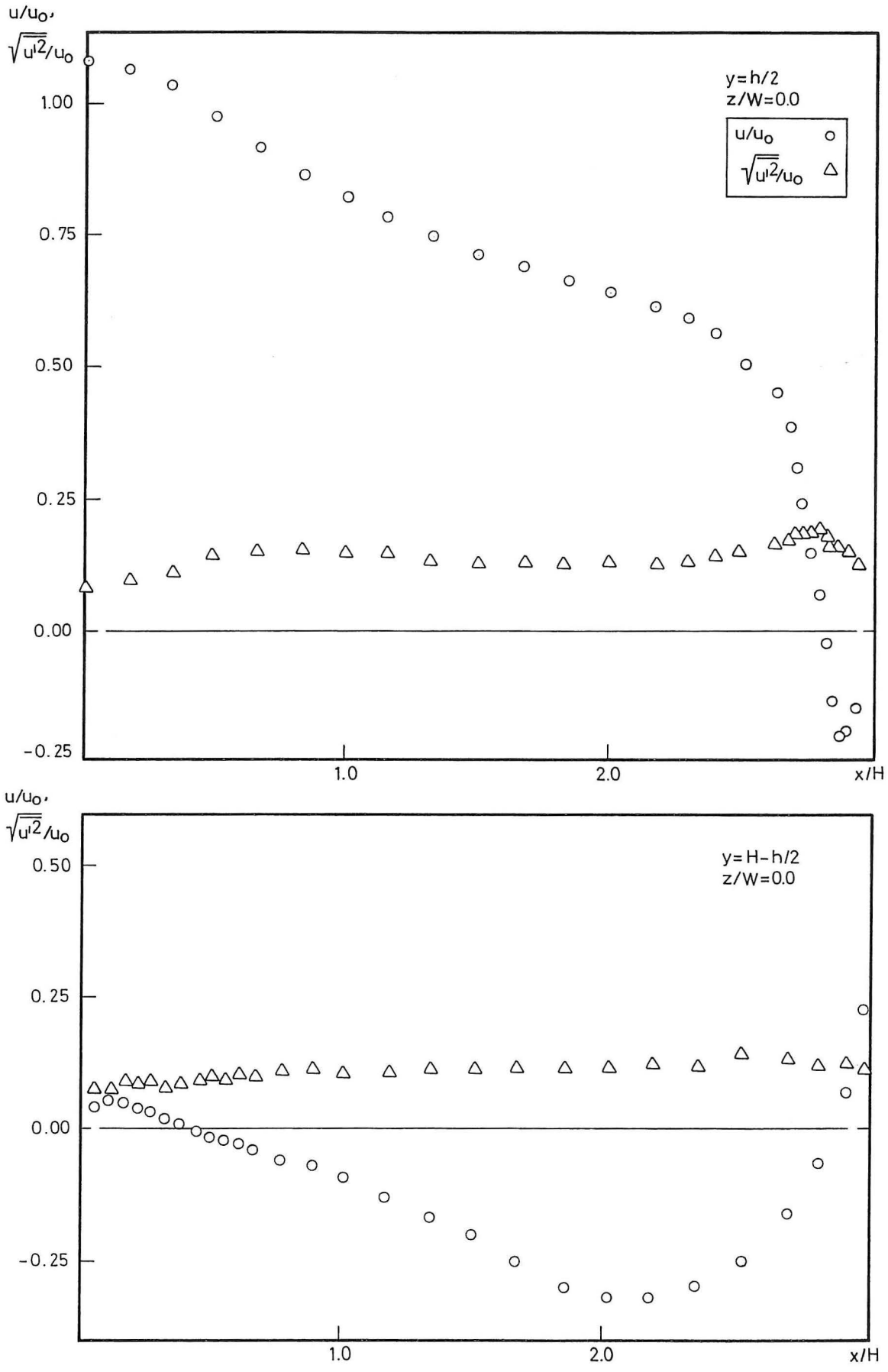

Figure 7. Mean and rms velocity near the top and bottom walls in the symmetry plane, $Re = 5000$, see [1].

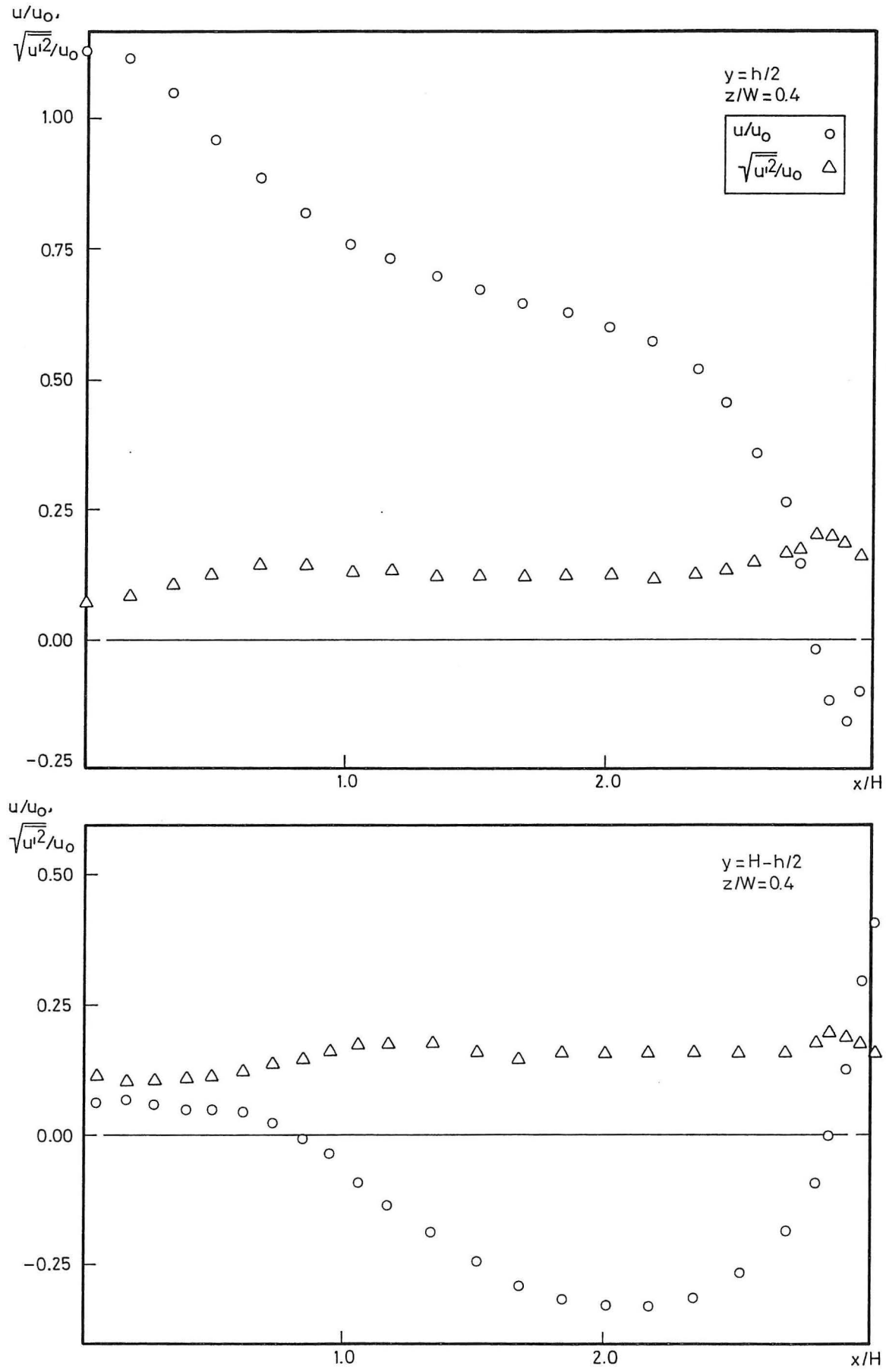

Figure 8. Mean and rms velocity near the top and bottom walls at $z/W = 0.4$, $Re = 5000$, see [1].

OTHER MEASUREMENTS

The measurements described in this chapter are made by hot-wire anemometry, pitot tube and thermocouples in a model with the following geometrical specification, see [2]

$$h/H = 0.056\ ,\ L/H = 3.0\ ,\ t/H = 0.16$$

$$W/H = 4.7,\ 1.0\ \textit{and}\ 0.5 \tag{15}$$

The model has a real size of $H = 127$ mm.

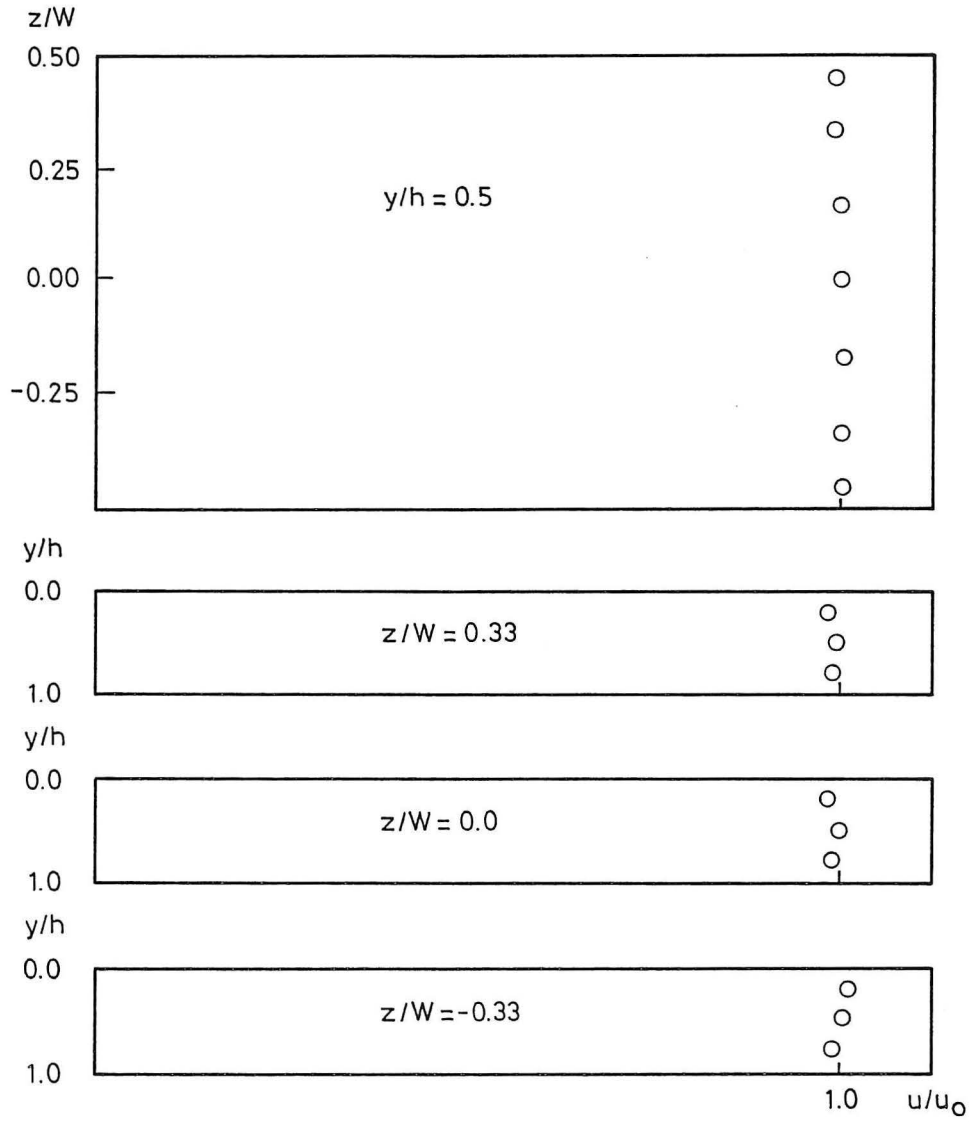

Figure 9. Velocity distribution at the supply opening measured by pitot tube, Re = 5000, $W/H = 4.7$.

The velocity distribution in the supply opening is shown in figure 9. The velocity is rather constant across the whole area of the slot.

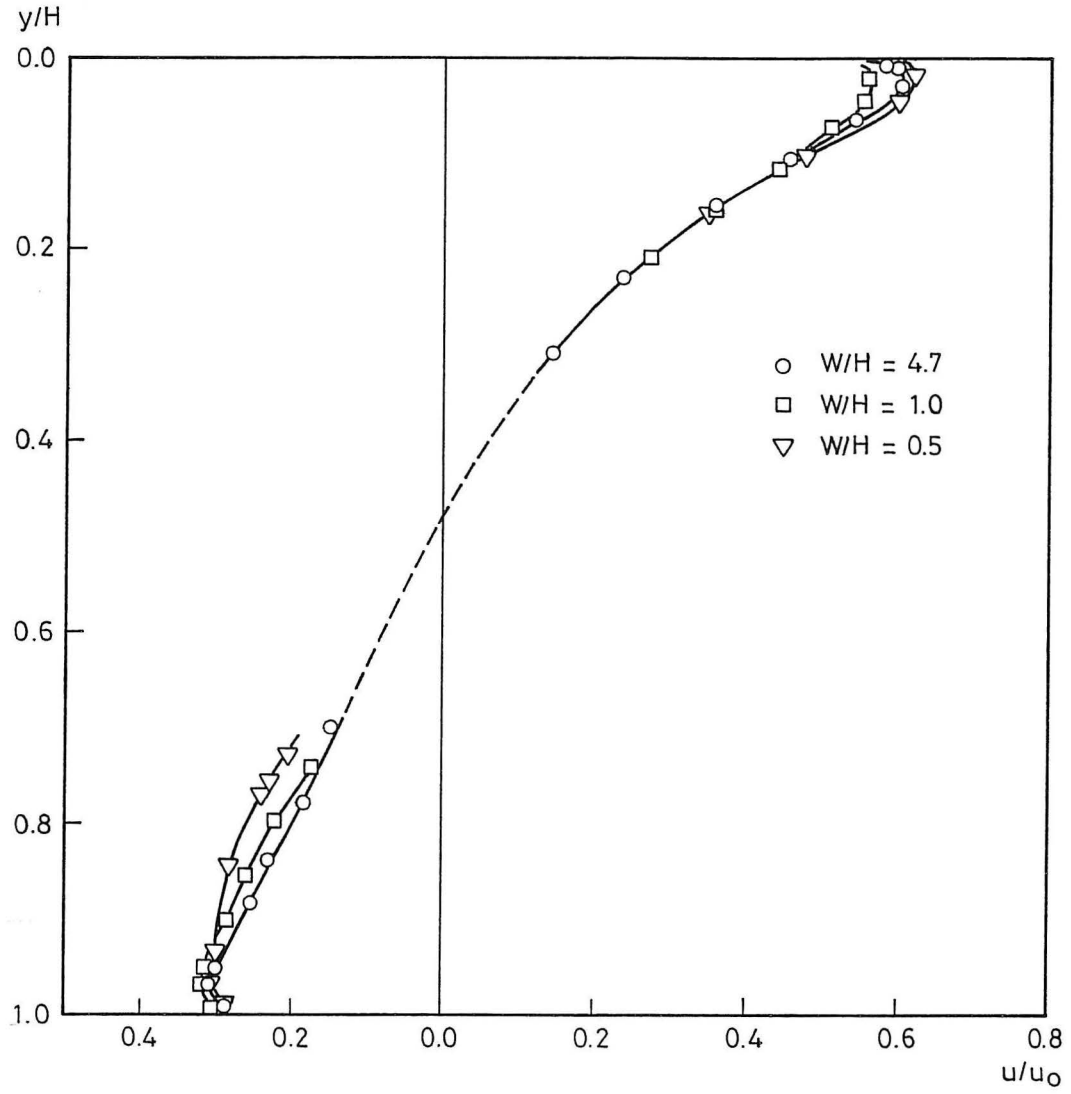

Figure 10. Hot-wire measurements of mean velocity at $x/H = 2.0$ and $z/W = 0$ for three different widths of the model, $Re = 7100$, see [2].

Figure 10 shows the influence of the width W. The measurements suggest three-dimensional flow but it is not possible to exclude some influence from the probe support due to the small width of the model. It is difficult to compare the results with measurements in the last chapter because the inlet profiles are slightly different in the two cases. Figure 10 shows a large area in the middle of the flow where hot-wire measurements of mean velocity are impossible.

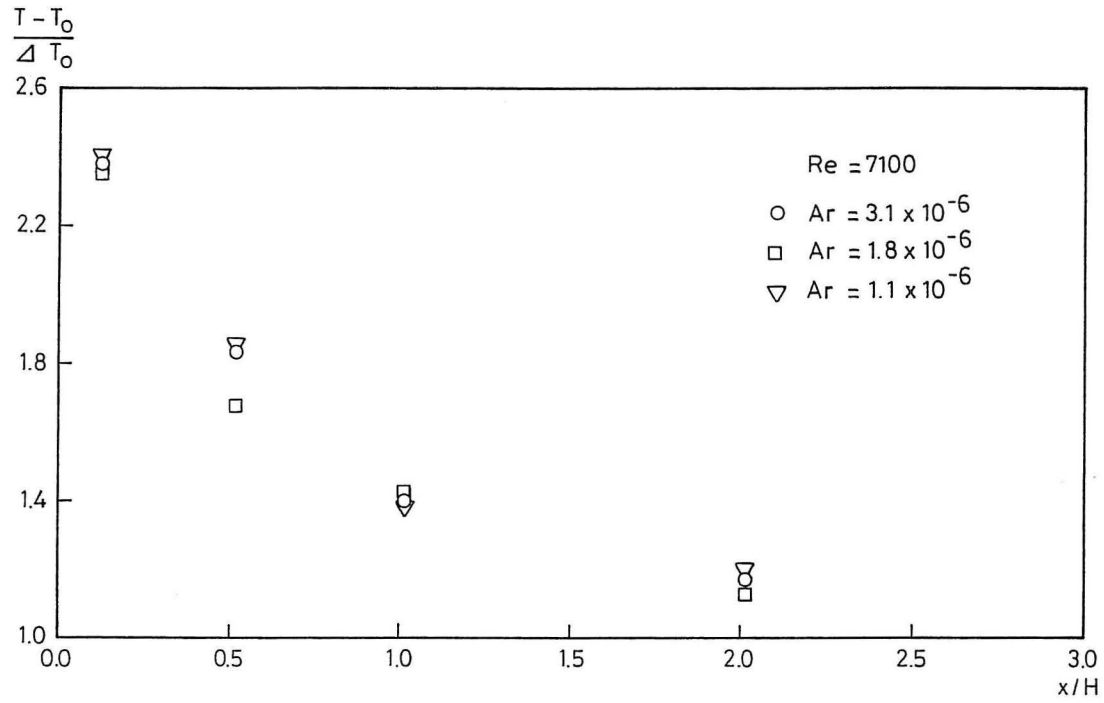

Figure 11. Measured temperature distribution at $y/H = 0.75$ and $z/W = 0.17$ in model with heat flux through the bottom surface, $Re = 7100$, $W/H = 4.7$, see [2].

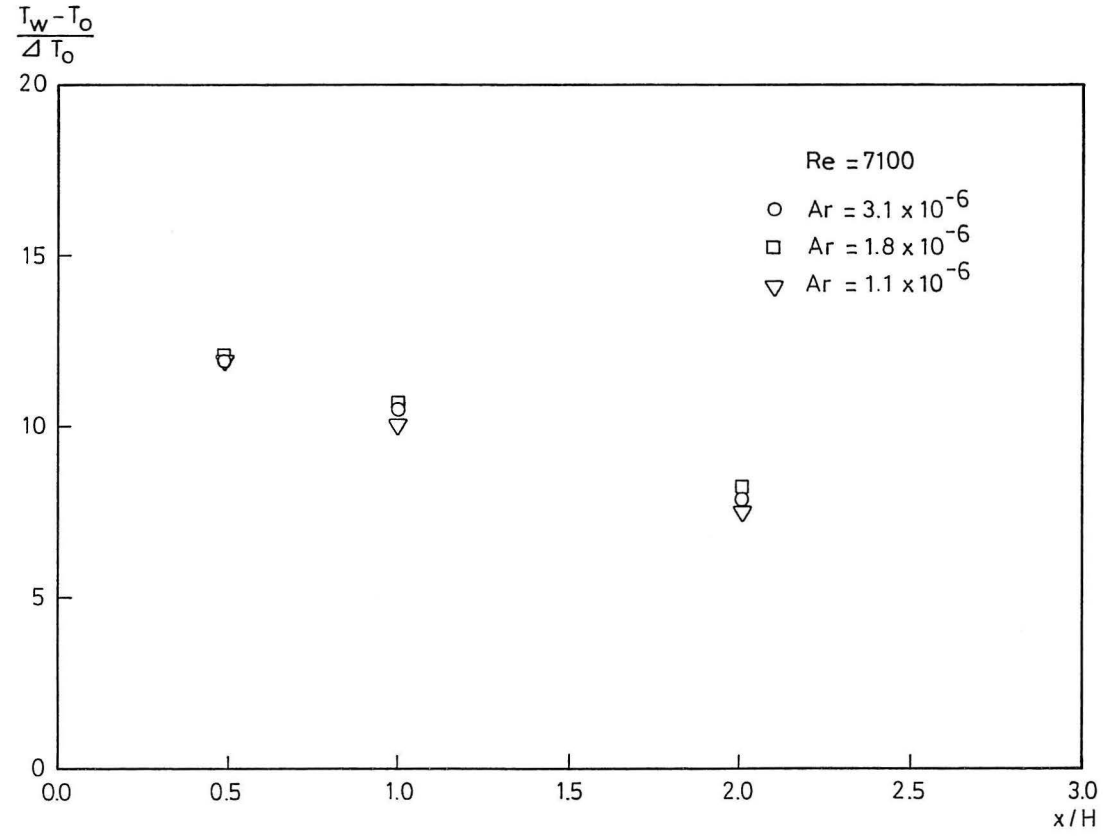

Figure 12. Measured temperatures T_w at the bottom surface in the experiment shown in figure 11.

Figures 11 and 12 show the air temperature and surface temperature measured in an experiment with heat flux through the bottom surface.

The Archimedes numbers in the experiments are small and the velocity distribution will therefore be similar to the measurements shown in figure 10.

It is difficult to produce a constant heat flux in the experiment but comparisons between predictions with different heat flux distributions at the bottom surface show an insignificant influence on the temperature profile at $y/H = 0.75$.

REFERENCES

[1] Restivo, A., Turbulent Flow in Ventilated Rooms, Ph.D. thesis, University of London, March 1979.

[2] Nielsen, P.V., Flow in Air Conditioned Rooms (English translation of Ph.D. thesis, Technical University of Denmark, 1974), Danfoss A/S, Denmark, 1976.

[3] Nielsen, P.V., A. Restivo and J.H. Whitelaw, The Velocity Characteristics of Ventilated Rooms, Journal of Fluids Engineering, September 1978, Vol. 100, pp. 291-298.

[4] Davidson, L. and E. Olsson, Calculation of some Parabolic and Elliptic Flows using a new One-Equation Turbulence Model, Proc. 5th International Conference on Numerical Methods in Laminar and Turbulent Flow, Montreal, Vol. 1, 1987.

[5] Schwenke, H., Über das Verhalten ebener horizontaler Zuluftstrahlen im begrenzten Raum, Luft- und Kältetechnik, No. 5, Dresden, 1975.

[6] Nielsen, P.V., A. Restivo an J.H. Whitelaw, Buoyancy-Affected Flows in Ventilated Rooms, Numerical Heat Transfer, Vol. 2, pp. 115-127, 1979.